Available online at www.sciencedirect.com
ScienceDirect
International Journal of Heat and Mass Transfer 50 (2007) 1855–1864
International Journal of HEAT and MASS TRANSFER
www.elsevier.com/locate/ijhmt

Numerical study of fluid flow and heat transfer in microchannel cooling passages

Jiang-Tao Liu [a], Xiao-Feng Peng [a], Wei-Mon Yan [b,*]

[a] Laboratory of Phase Change and Interfacial Transport Phenomena, Department of Thermal Engineering, Tsinghua University, Beijing 100084, China
[b] Department of Mechatronic Engineering, Huafan University, Shih Ting, Taipei 22305, Taiwan, ROC

Received 29 June 2006; received in revised form 4 October 2006
Available online 30 November 2006

Abstract

Numerical investigation was conducted for fluid flow and heat transfer in microchannel cooling passages. Effects of viscosity and thermal conductivity variations on characteristics of fluid flow and heat transfer were taken into account in theoretical modeling. Two-dimensional simulation was performed for low Reynolds number flow of liquid water in a 100 μm single channel subjected to localized heat flux boundary conditions. The velocity field was highly coupled with temperature distribution and distorted through the variations of viscosity and thermal conductivity. The induced cross-flow velocity had a marked contribution to the convection. The heat transfer enhancement due to viscosity-variation was pronounced, though the axial conduction introduced by thermal-conductivity-variation was insignificant unless for the cases with very low Reynolds numbers.

Keywords: Convection; Microchannel; Temperature-dependent property; Flow entrance effect

1. Introduction

The application of microchannel heat sinks is drawing increasing attentions as one of the most promising high-efficiency heat exchange technologies in, e.g., the cooling of electronic devices, automotive heat exchangers, laser process equipments, and aerospace technology, etc. Microchannel flow and heat transfer has become an quite active thermal and fluid research field since the early work of Tuckerman and Pease [1], and Wu and Little [2,3]. Intensive investigations were performed experimentally and theoretically in the following decades [4–10], which were categorized into various topics and elaborately summarized in the comprehensive review of Sobhan and Garimella [11]. The friction factor and heat transfer coefficient were the most concerned parameters in the literature, whose derivation from classical theory and the dependency on the channel diameter were not conclusive due to the different or even contradictory suggestions provided by different investigators [12].

Besides the reasonable suspect on the quality of measured data, several possible explanations were provided for the derivations from classical theory, or so-called microscale effects. Some attributed the derivations to wall roughness, since the same absolute surface roughness has enlarged effect on small diameter channels than on large ones, as in the work of Kandlikar et al. [13]. Some introduced the electric double-layer (EDL) effect, as in Yang et al. [14], and in Ng and co-worker [15,16], as a body force term in the momentum equation to obtain the Nusselt number and friction factor for an aqueous solution of low ionic concentration and a wall surface of high zeta potential. However, it was also noted that for the conditions used in the evaluation of the model, EDL effects should not be important for pressure drop or heat transfer in channels larger than 40 μm.

Flow development of hydraulic and thermal boundary layers is considered important in microchannel convections, which are often characterized by laminar flow.

* Corresponding author. Tel.: +886 2 2663 2102; fax: +886 2 2663 1119.
E-mail address: wmyan@huafan.hfu.edu.tw (W.-M. Yan).

0017-9310/$ - see front matter © 2006 Elsevier Ltd. All rights reserved.
doi:10.1016/j.ijheatmasstransfer.2006.10.004

Nomenclature

Br_{qw}	Brinkman number based on wall heat flux
Br_{Sk}	modified Brinkman number based on viscosity-temperature sensitivity
$Br_{S\mu}$	modified Brinkman number based on thermal-conductivity-temperature sensitivity
D	channel width
Eu	Euler number
L	length
Nu	local Nusselt number
P	dimensionless pressure
Pe	Peclet number
Pr	Prandtl number
R_{conv}	ratio of mean transverse to axial convection
Re_D	Reynolds number
S_k	thermal-conductivity-temperature sensitivity
S_μ	viscosity-temperature sensitivity
T	temperature
U	dimensionless main-flow velocity
W	dimensionless cross-flow velocity
X	non-dimensionalized axial coordinate by D
X^+	non-dimensionalized axial coordinate by D and Re_D
Z	non-dimensionalized transverse coordinate by D
c_p	specific heat
h	heat transfer coefficient
k	thermal conductivity
p	pressure
p_a	atmosphere pressure
q''_w	wall heat flux
u	main-flow velocity
w	cross-flow velocity
x	axial coordinate
z	transverse coordinate

Greek symbols

Φ	viscous dissipation term
θ	dimensionless temperature
μ	viscosity
ρ	density

Superscript

*	dimensionless form of selected parameter

Subscripts

0	inlet property
CP	constant property
DN	downstream region
FD	fully developed flow
H	heated region
UP	upstream region
b	bulk
m	mean
w	wall

Fedorov and Viskanta [17] reported a substantial developing flow effect in the channels from their three-dimensional numerical simulations. Similar conclusion was drawn in the numerical investigation of Qu and Mudawar [18]. Their most recent work [19], collaborated with other authors, conducted experimental and computational studies on flow development and pressure drop for adiabatic single-phase water flow in a single 222 μm wide, 694 μm deep, and 12 cm long rectangular microchannel at Reynolds numbers ranging from 196 to 2215. The velocity field was measured using a microparticle image velocimetry system. Pronounced flow field evidence was provided for the strong entrance effect from their experiments and numerical simulations. Gamrat et al. [20] performed both two- and three-dimensional numerical analysis of microchannel convection, considering the thermal entrance effects and conjugate heat transfer of fluid and solid wall. The results of their numerical simulation confirmed, together with those mentioned above, that the continuum model of conventional mass, Navier–Stokes and energy equations are of adequate accuracy in representing the microchannel flow and heat transfer characteristics.

As mentioned above, constant thermophysical properties were usually used in the analyses of previous work. They could not fully reveal the characteristics of fluid flow and heat transfer in the conditions of high heat flux and low Reynolds number flow, implying large variation of liquid properties, which is always encountered in the applications of microchannels. For water in the temperature range from 0 to 100 °C, μ varies by 84% (decrease), k by 21% (increase), ρ by 4% (decrease) and c_p by 1% (non-monotonic). [21]. The relatively large variations of μ and k indicate that the two properties should be treated as functions of temperature. As a result, the energy equation is no longer independent of the momentum equation in the conservative model, drawing significant difficulty in the theoretical analysis. The property-ratio method [22] was introduced and was popularly employed to the correction of Nusselt number for convection in convectional tubes, which fails to provide reasonable prediction for large heat flux. Mahulikar and Herwig [23] established a continuum-based model for laminar convections, incorporating temperature dependence of fluid viscosity and thermal conductivity. The solution of the model relied on mature computational fluid dynamics technology and showed applicability for a large range of heat flux, indicating its suitable usage in microchannel convections. In their most recent work [24], detailed effects of temperature-dependent properties were provided on the fully developed laminar microconvection in circular tubes.

Non-uniform heating conditions are another important feature in the practical operation of microchannel devices in terms of both space and time scales. It was usually assumed, however, uniform thermal boundary in the previous studies, as either isothermal or uniform heat flux condition. The non-uniformity of thermal boundary conditions should remarkably alter the temperature distribution of the fluid, and additionally alter the flow field through the variation of μ and k.

The present work numerically investigated the two-dimensional low Reynolds number convection of water in microchannel with the combination of locally heated wall boundary condition and temperature-dependent viscosity and thermal conductivity of liquid water. Heat transfer performance was evaluated by comparing with constant–property solutions. The effect of thermal development and property variation was discussed through detailed analysis of local momentum and heat transport.

2. Fundamental considerations

The model is derived from continuum-based conservation equations of mass, momentum and energy [25], with the following several basic assumptions:

(1) Steady laminar flow.
(2) Incompressible Newtonian fluid.
(3) Constant specific heat of the fluid.
(4) Thermal conductivity and viscosity are the single variable functions of temperature.
(5) Negligible effect of gravity and other forms of body forces.

The resulting governing equations are:

Continuity equation

$$\nabla \cdot \mathbf{u} = \mathrm{div}\,\mathbf{u} = 0 \tag{1}$$

Momentum equation

$$\rho(\mathbf{u}\cdot\nabla)\mathbf{u} = -\nabla p + \mu\nabla^2\mathbf{u} + S_\mu \nabla T \cdot \mathrm{def}\,\mathbf{u} \tag{2}$$

Energy equation

$$\rho c_p(\mathbf{u}\cdot\nabla)T = k\nabla^2 T + S_k \nabla T\cdot\nabla T + \Phi \tag{3}$$

where $S_\mu = \mathrm{d}\mu/\mathrm{d}T$, the viscosity-temperature sensitivity; $S_k = \mathrm{d}k/\mathrm{d}T$, the thermal-conductivity-temperature sensitivity; $\Phi = \mu\mathrm{def}\,\mathbf{u}{:}\mathrm{def}\,\mathbf{u}/2$, the viscous dissipation term; $\mathrm{def}\,\mathbf{u} = \nabla\mathbf{u} + (\nabla\mathbf{u})^{\mathrm{T}}$, the rate of deformation tensor.

By restricting the discussion within two-dimensional space, and applying the following dimensionless groups:

$$\begin{aligned}
&\mathbf{R} = X\mathbf{e}_i + Z\mathbf{e}_k = \mathbf{r}/D = x/D\mathbf{e}_i + z/D\mathbf{e}_k,\\
&\mathbf{U} = U\mathbf{e}_i + W\mathbf{e}_k = \mathbf{u}/u_0 = u/u_0\mathbf{e}_i + w/u_0\mathbf{e}_k\\
&\theta = \frac{k_0(T-T_0)}{q''_{\mathrm{w}}D}, \quad k^* = k/k_0, \quad \mu^* = \mu/\mu_0,\\
&P = p/p_a, \quad S^*_\mu = S_\mu/S_{\mu,0}, \quad S^*_k = S_k/S_{k,0}
\end{aligned} \tag{4}$$

the governing equations are then non-dimensionalized as follows:

Continuity equation

$$\frac{\partial U}{\partial X} + \frac{\partial W}{\partial Z} = 0 \tag{5}$$

X-component momentum equation

$$\begin{aligned}
&U\frac{\partial U}{\partial X} + W\frac{\partial U}{\partial Z}\\
&\quad = -Eu\frac{\partial P}{\partial X} + \frac{\mu^*}{Re_D}\left(\frac{\partial^2 U}{\partial X^2} + \frac{\partial^2 U}{\partial Z^2}\right)\\
&\qquad + \frac{1}{Re_D}\frac{Br_{S\mu}}{Br_{qw}}S^*_\mu\left[2\frac{\partial\theta}{\partial X}\frac{\partial U}{\partial X} + \frac{\partial\theta}{\partial Z}\left(\frac{\partial U}{\partial Z} + \frac{\partial W}{\partial X}\right)\right]
\end{aligned} \tag{6}$$

Z-component momentum equation

$$\begin{aligned}
&U\frac{\partial W}{\partial X} + W\frac{\partial W}{\partial Z}\\
&\quad = -Eu\frac{\partial P}{\partial Z} + \frac{\mu^*}{Re_D}\left(\frac{\partial^2 W}{\partial X^2} + \frac{\partial^2 W}{\partial Z^2}\right)\\
&\qquad + \frac{1}{Re_D}\frac{Br_{S\mu}}{Br_{qw}}S^*_\mu\left[\frac{\partial\theta}{\partial X}\left(\frac{\partial W}{\partial X} + \frac{\partial U}{\partial Z}\right) + 2\frac{\partial\theta}{\partial Z}\frac{\partial W}{\partial Z}\right]
\end{aligned} \tag{7}$$

Energy equation

$$\begin{aligned}
&U\frac{\partial\theta}{\partial X} + W\frac{\partial\theta}{\partial Z}\\
&\quad = \frac{1}{Re_D Pr}\left\{k^*\left(\frac{\partial^2\theta}{\partial X^2} + \frac{\partial^2\theta}{\partial Z^2}\right) + \frac{Br_{Sk}}{Br_{qw}}S^*_k\left[\left(\frac{\partial\theta}{\partial X}\right)^2 + \left(\frac{\partial\theta}{\partial Z}\right)^2\right] + \Phi^*\right\}
\end{aligned} \tag{8}$$

where the Φ^* stands for the viscous dissipation term

$$\Phi^* = Br_{qw}\mu^*\left[2\left(\frac{\partial U}{\partial X}\right)^2 + 2\left(\frac{\partial W}{\partial Z}\right)^2 + \left(\frac{\partial W}{\partial X} + \frac{\partial U}{\partial Z}\right)^2\right] \tag{9}$$

and the dimensionless governing parameters are defined as

$$\begin{aligned}
&Re_D = \frac{\rho u_0 D}{\mu_0}, \quad Pr = \frac{c_p\mu_0}{k_0}, \quad Eu = \frac{p_a}{\rho u_0^2},\\
&Br_{qw} = \frac{u_0^2\mu_0}{q''_{\mathrm{w}}D}, \quad Br_{S\mu} = \frac{S_{\mu,0}u_0^2}{k_0}, \quad Br_{Sk} = \frac{S_{k,0}\mu_0 u_0^2}{k_0^2}
\end{aligned} \tag{10}$$

The Br_{qw} is the Brinkman number based on wall heat flux, $Br_{S\mu}$ is modified Brinkman number based on viscosity-temperature sensitivity, and Br_{Sk} is modified Brinkman number based on thermal-conductivity-temperature sensitivity. In the dimensionless form of conservative equations, Br_{qw} appears as a multiplier to the viscosity dissipation term, while its reciprocal appears before the temperature terms that determine the significance of variation in fluid properties. When Br_{qw} is about the value of or even larger than unity, the momentum transfer across flow is

comparable to heat transfer from wall, and momentum transfer results in significant viscous dissipation [26]. When $Br_{qw} \ll 1$, the coupling effect of energy transport on momentum transport increases through the variation of μ. Thus for a typical application of microchannels, high heat flux and low flow velocity always result in small value of Br_{qw}, which indicates strong influence of property variation on the convection. $Br_{S\mu}$ and Br_{Sk} show the relative importance of momentum transport across the flow due to viscosity and thermal-conductivity variation, over the energy transport due to the fluid conduction, respectively. Elaborated physical significances of the Brinkman numbers could be found in Mahulikar and Herwig [23].

Water is used as working liquid in this simulation. The viscosity and thermal conductivity are calculated by the IAPWS-IF97 method [21] in the temperature range of liquid water, i.e., from 0 to 100 °C.

The governing equations are solved in the domain shown in Fig. 1. Taking the advantage of symmetry, only half of the channel is modeled. The channel wall is divided into three sections. The center region is heated at constant heat flux, q''_w, while the upstream and downstream regions are adiabatic walls. The length of heated region is fixed at $20D$. The lengths of upstream and downstream region are both set as $10D$, which are selected based on a compromise between computation cost and the requirement for numerical stability. No slip condition is set for all the three sections. The origin of the two-dimensional rectangular coordinate system is located at the start point of heated region on the centerline (symmetric plane), with the x-axis running along the channel.

At the entrance ($X = -10$), the fully-developed flow condition is assumed with uniform temperature, given as

$$U = 1.5(1 - 4Z^2) \tag{11a}$$

$$W = 0 \tag{11b}$$

$$\theta = 0 \tag{11c}$$

At the exit ($X = 30$), the axial gradients for all the transport variables except pressure are assumed to be zero.

The influence of the μ- and k-variations on the local heat transfer in a microchannel is the focused issue in present work. Thus, the local Nusselt number is an important parameter, defined as

$$Nu = \frac{hD}{k_m} = \frac{q''_w D}{k_m(T_w - T_b)} = \frac{1}{k^*_m(\theta_w - \theta_b)} \tag{12}$$

where the dimensionless wall and bulk temperatures are defined as follows:

$$\theta_w = \frac{k_0(T_w - T_0)}{q''_w D}, \quad \theta_b = \frac{k_0(T_b - T_0)}{q''_w D} = \int_0^1 U\theta \, dZ \tag{13}$$

In order to examine the effects of property variation more apparently, the relative difference of local Nu for variable–property and constant–property is defined as follows:

$$\Delta Nu\% = \frac{Nu - Nu_{CP}}{Nu_{CP}} \times 100\% \tag{14}$$

3. Numerical method and validation

The governing equations with boundary conditions were solved by the commercial CFD code, CFX5. The equations were discretized by means of a fully implicit second order finite volume method with modified upwind advection scheme. In this work, the grid points used in the x and z directions were selected to be 600 and 70, respectively, with carefully distributed density near central heated region. To obtain better accuracy in the numerical computations, coarse and fine grid systems were considered in the preliminary tests. Effects of the grid number on the predictions of local Nusselt number are shown in Table 1. The maximum deviations among the computations on the grids of 240×50, 600×50, 600×70, 600×100 and 900×70 were less than 0.014%. Therefore, the grid system of 600×70 points seemed to be sufficient to resolve the behaviors of

Table 1
Comparison of the local Nusselt number Nu for various grid points at $q''^*_w = 0.513$

Grid ($X \times Z$)	Location X			
	5	10	15	19
240×50	5.6369	4.8571	4.5663	4.4541
600×50	5.6370	4.8572	4.5663	4.4542
600×70	5.6362	4.8566	4.5659	4.4538
600×100	5.6358	4.8563	4.5657	4.4536
900×70	5.6362	4.8566	4.5659	4.4538

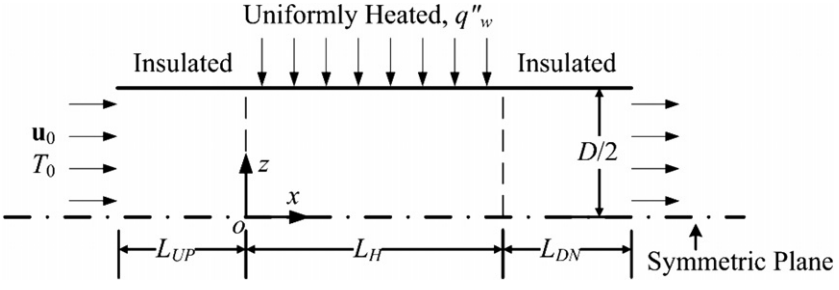

Fig. 1. Schematic diagram of the physical system.

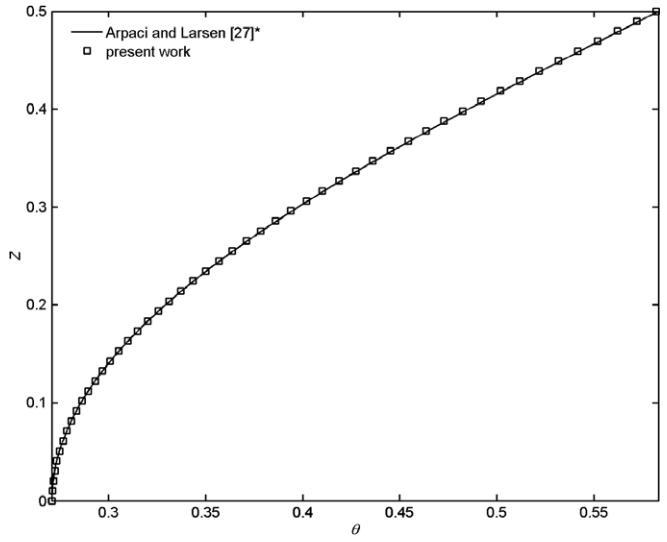

Fig. 2. θ–Z profile from present work and analytic solution. (*Manipulated in consistence with the definition of θ in the present work.)

the fluid flow and heat transfer in microchannels. A converged solution was obtained using this grid, with root mean square residuals less than 10^{-7} for all the transport variables and independent of the iteration numbers, and domain imbalances of mass, momentum and energy conservation less than 10^{-7}. The validation of the numerical method was performed using water with constant properties and uniform heat flux condition over the entire channel wall, as a benchmark case. The temperature profile at fully-developed region of the channel was compared with analytical solution, which showed excellent agreement, as depicted in Fig. 2. The Nusselt value obtained from simulation agreed with the theoretical value, $Nu_{\mathrm{CP,FD}} = 70/17$ [27] with an relative error lower than 0.05%. Apparently, the solution method and the formulation adopted were appropriate for the present study.

So far the present numerical method was proved reliable for the type of two-dimensional microchannel flow and heat transfer problem described above. A series of simula-

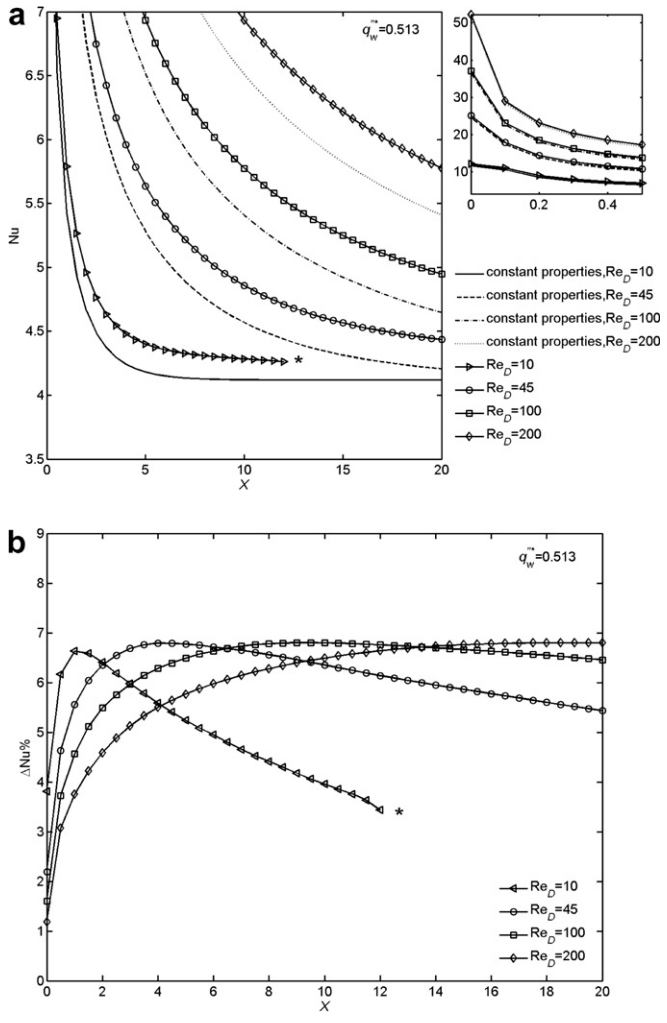

Fig. 3. Effects of Reynolds number Re_D at $q''^*_{\mathrm{w}} = 0.513$ on local Nusselt number with or without properties variations. (a) Local Nu and (b) local $\Delta Nu\%$ with X.

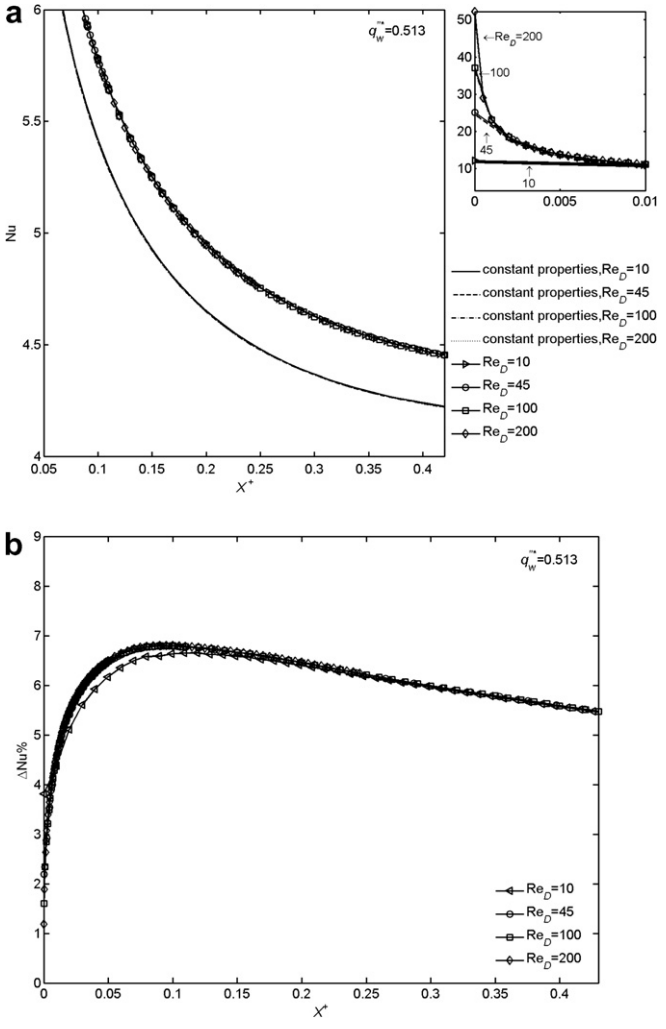

Fig. 4. Effects of Reynolds number Re_D at $q''^*_{\mathrm{w}} = 0.513$ on local Nusselt number with or without properties variations. (a) Local Nu and (b) local $\Delta Nu\%$ with X^+.

tions were then carried out with converged results obtained using this method at variable conditions, as discussed in the next section.

4. Results and discussion

For all tested cases in this work, the channel width, D, was 100 μm, and inlet temperature, $T_0 = 20\ ^\circ\mathrm{C}$. The Reynolds number, Re_D and heat flux were varied to examine the effects of property variation within the temperature range of liquid water. For the convenience of comparison with other researches, the heat flux was non-dimensionalized as the following form:

$$q''^{*}_{\mathrm{w}} = \frac{q''_{\mathrm{w}} D}{k_0 T_0} \tag{15}$$

which ranged from 0.057 to 0.855 in the present study.

4.1. Role of Reynolds number

Typical local Nu distributions for variable Re_D at a specified heat flux are shown in Fig. 3(a). The curves with different line styles correspond to different Re_D for constant–property water, while the curves with markers refer to those for variable–property water. The curves depart from each other even for the constant–property cases as Re_D varying from 10 to 200. For higher Re_D, the Nu jumps to a higher value at the front of heated region, and then decays to $Nu_{\mathrm{CP,FD}}$ within a longer distance downstream. The variable–property curves are always higher than their constant–property counterparts. Note that the variable–property curve for $Re_D = 10$ is truncated at $X \approx 12$ for inaccurate calculation, because after this location the fluid temperature is beyond 100 °C and thermophysical properties of liquid water are no longer available. The constant–property curve is not affected by this problem anyway, since the properties at $T_0 = 20\ ^\circ\mathrm{C}$ are used in the computation.

Fig. 3(b) shows the distributions of the $\Delta Nu\%$ along X for variable Re_D at a specified heat flux. It is clear that each curve indicates an increase in the Nu enhancement and a drop downstream. Both the peak location and the slope of the curve vary with Re_D, which may lead to a seemingly valid conclusion that $\Delta Nu\%$ is a function of X and Re_D, for a specified heat flux and working liquid. It is described as 'seemingly', because the curves in Fig. 3(b) are quite similar with each other, with almost same peak value and same trend. Inspired by the classical reduction method of entrance problem [28], the dimensionless abscissa $X^+ = X/Re_D = x/(DRe_D)$ is introduced, and the Nu and $\Delta Nu\%$ curves are expressed as its functions, as shown in Fig. 4.

As expected, the constant–property curves coincide with each other in most part of the heated region, except for the short starting area (See the small image in the upper-right of Fig. 4a). The small length of a departure near the start-

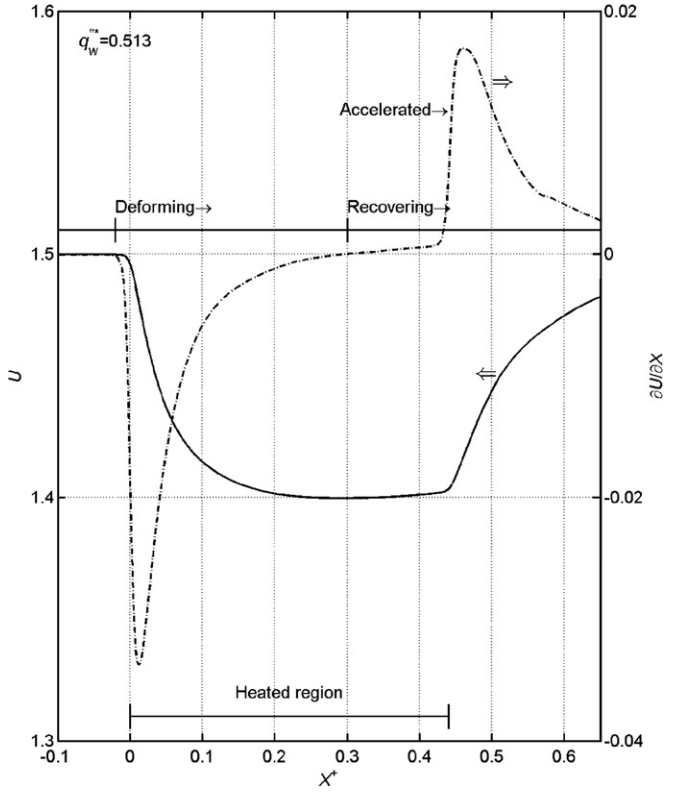

Fig. 5. Variations of main-flow velocity U and its streamwise gradient at $q''^{*}_{\mathrm{w}} = 0.513$.

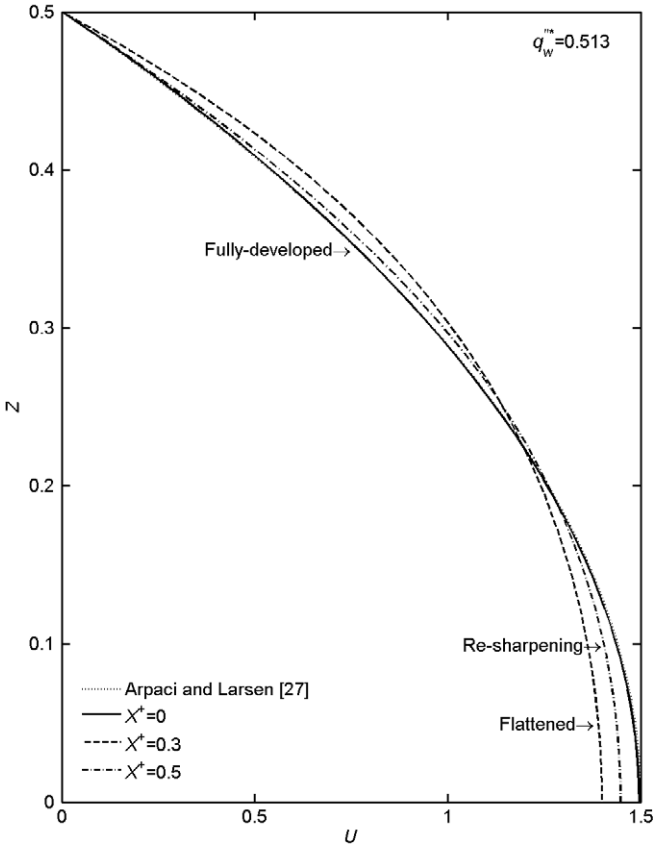

Fig. 6. Distributions of main-flow velocity U at different streamwise locations and $q''^{*}_{\mathrm{w}} = 0.513$.

ing point of heated region is mainly due to the axial fluid heat conduction, whose significance increases with a decreasing Re_D. The variable–property data, on the other hand, overlap to form another curve, which departs from the constant–property curve at a distance varying with X^+. The $\Delta Nu\%$ distributions show this phenomenon more directly that a single curve is formed, indicating the same heat transfer enhancement along X^+ at a specified heat flux. It turns out that $\Delta Nu\%$ is not the functions of X and Re_D separately, but their quotient. This fact implies that, on the functionary aspect, the variable–property mechanism performs as an amplifier of thermal development. The variable–property flow behavior, however, is quite different from constant–property developing flow, as elaborated in the following section.

4.2. Flow field characteristics and enhancement mechanism

The streamwise development of main-flow velocity, U, and its gradient is drawn at the centerline of the channel (symmetric plane) in Fig. 5. Since the fully-developed flow condition is given at the domain inlet, the centerline velocity keeps the value of 1.5 for $X^+ < 0^-$. When the flow enters the heated region, due to high heat flux, dramatic spacial μ-variation takes place and distorts the parabolic U–Z profile. The distorted profile varies together with temperature profile as the fluid heated along the flow until it achieves a most flattened profile. Afterward the flow undergoes a slow recovering process towards the parabolic profile until it leaves the heated region and accelerates to achieve fully developed flow at the absence of heating (see Fig. 6).

The cross-flow velocity component, W, is induced during the U variation process, out of necessity to satisfy the local mass conservation (Eq. (5)). Since this mechanism is originated from heat input, it is reasonable to infer that for a higher q''^*_w, a larger W is induced at a given streamwise location, which is proved in Fig. 7. The sign of W is always positive in the U-deforming part of heated region, since the flattened U profile forces an outward cross-section flow to the channel wall, which forms transverse convection as an enhancement to the heat removal from the wall. Though the entire scope of W is a small faction of U, the transverse convection is not negligible, contrary to popular belief, since the W is weighted by the cross-flow temperature gradient in the term of transverse convection, $W(\partial\theta/\partial Z)$ in Eq. (8). Hereby, the ratio of mean transverse to axial convection is defined as

$$R_{\text{conv}} = \left(\int_0^{0.5} W\frac{\partial\theta}{\partial Z}\,\mathrm{d}Z\right) \Big/ \left(\int_0^{0.5} U\frac{\partial\theta}{\partial X}\,\mathrm{d}Z\right) \tag{16}$$

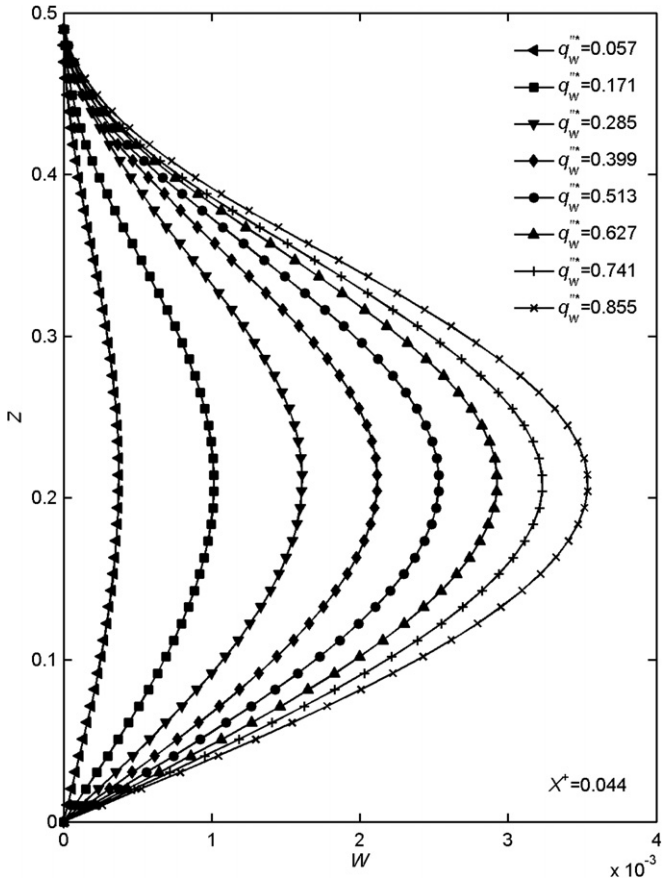

Fig. 7. Effects of heat flux q''^*_w on distributions of cross-flow velocity W at X^+=0.044.

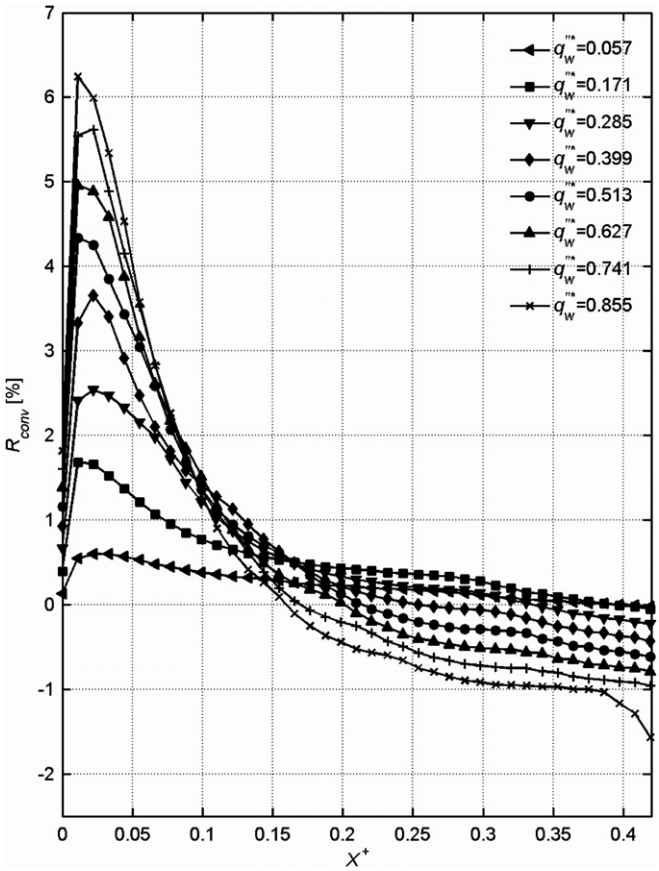

Fig. 8. Effects of heat flux q''^*_w on distributions of R_{conv}.

R_{conv} is calculated and presented in Fig. 8 for different heat fluxes. Obviously, for a typical case ($q''^{*}_{w} = 0.513$), a peak value of 4.3% is achieved at the vicinity of heated region front. The value of R_{conv} declines downstream to be zero at the position of largest U deformation, and then keeps going down to be minus (due to minus value of W, inward flow away from the channel wall) near the end of heated region. For higher q''^{*}_{w}, R_{conv} increases to a higher peak value, yet decreases more dramatically along the flow. For a small q''^{*}_{w}, in contrast, R_{conv} keeps to be a small positive value until the very last part of heated region.

Figs. 9 and 10 depict the Nu and $\Delta Nu\%$ distributions, respectively, at different dimensionless wall heat fluxes, through which the effect of temperature-dependent viscosity is pronounced. It is found that the maximum $\Delta Nu\%$ obtained in present work is as large as 10% over the constant–property Nu, which should not be neglected. This can be made plausible by noting the fact that the axial convection contributes to the enhancement of heat transfer, due to enlarged U–Z gradient for distorted U profile. It is worth noting that all the flow characteristics discussed in this section are unique for variable–property cases, due to the coupling mechanism from temperature field through μ-variation.

Even the temperature distribution itself, however, is not the same with constant–property thermal development,

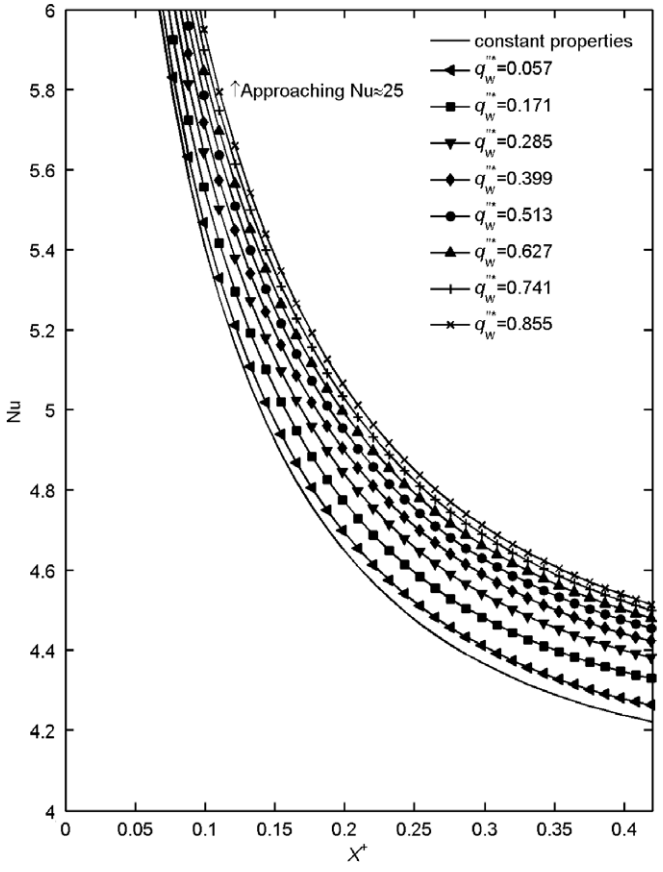

Fig. 9. Effects of heat flux q''^{*}_{w} on local Nusselt number Nu.

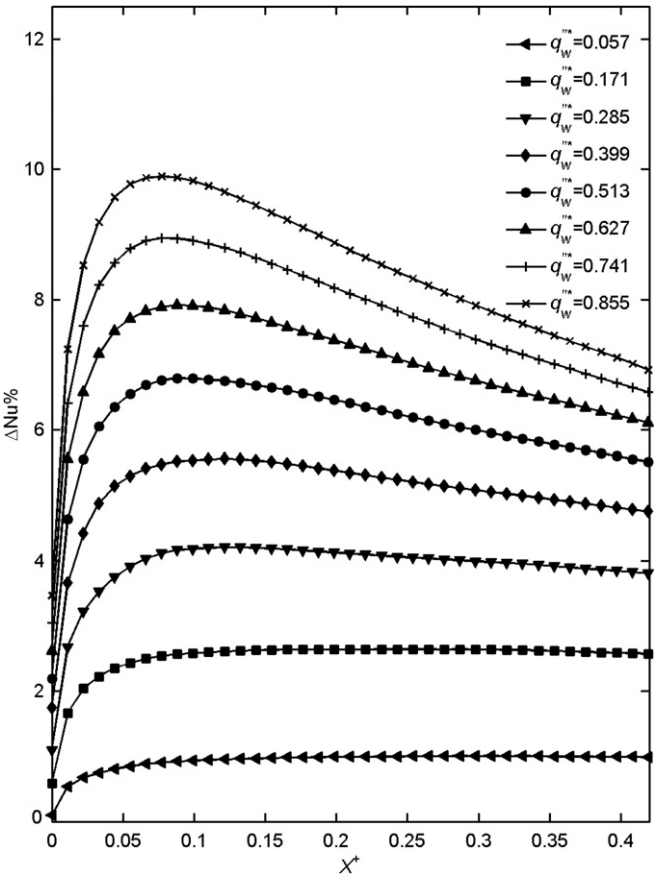

Fig. 10. Effects of heat flux q''^{*}_{w} on local $\Delta Nu\%$.

because of temperature-dependent thermal conductivity k. High temperature near the wall indicates higher k, which reversely promotes the heat removal from the wall and alters thermal diffusion. The k-variation along flow is also expected to affect the axial fluid conduction through the term in Eq. (8)

$$\frac{1}{Re_D Pr}\left\{k^*\frac{\partial^2\theta}{\partial Z^2}+\frac{Br_{Sk}}{Br_{qw}}S_k^*\left(\frac{\partial\theta}{\partial Z}\right)^2\right\}$$

which is derived from the $\frac{\partial}{\partial z}(k\frac{\partial T}{\partial z}) = k\frac{\partial^2 T}{\partial z^2}+\frac{\partial k}{\partial z}\frac{\partial T}{\partial z}$ term in dimensional energy equation. In the work of Mahulikar and Herwig [24], the discussions on the role of k-variation were mostly on the scene of constant heat flux wall condition, for which the temperature profile along flow is almost linear, implying negligible second derivative of temperature. The axial conduction is then determined by the product $(\partial k/\partial z)\cdot(\partial T/\partial z)$. Comparison between the effects of "μ- and k-variations", "μ-variation only" and "k-variation only" were performed, showing "direct" and more significant enhancement of Nu for k-variation than μ-variation. It is a common understanding that the relative significance of fluid axial conduction than convection varies with the product of Re and Pr, known as Peclet number in the literature. The Nu data that provided in [24], however, did not come along with Reynolds number specified, which weakened the persuasion of previously mentioned conclusion.

The concerned heat transfer performance in present work, on the other hand, is evaluated at the presence of thermally developing flow. The second derivative of temperature in the axial conduction term is no longer negligible due to nonlinear variation of temperature profile along flow. Actually, the effect of fluid axial heat conduction on Nu for thermal entrance flow is not streamwisely uniform, as discussed in Shan and London [28]. They concluded that for $Pe > 10$, the effect of fluid axial conduction was simply insignificant. The minimum Pe in present work is larger than 50 (larger than 200 in most cases). Thus it is not surprising that no k-variation influence is detectable in most cases of present work except for those at very low Reynolds numbers. (Note that the slight deviation of $Re_D = 10$ curve from the others at the starting part of heated region, as shown in Fig. 4b.)

5. Conclusion

Numerical investigation was conducted in an effort to perform an in-depth analysis for microchannel convections. Localized non-successive high heat flux boundary condition is frequently encountered in practical applications of microchannel heat exchangers, which results in steep temperature rise and dramatic property variation of working liquid in both flow and cross-flow directions. By considering liquid water of μ- and k-variation with temperature, two-dimensional convection in a $D = 100$ μm single channel was theoretically modeled and numerically solved for different heat flux and Reynolds numbers. The following conclusions could be drawn from the results.

1. The velocity field is highly coupled with temperature distribution and distorted through the variation of μ and k.
2. The induced cross-flow velocity W has non-negligible contribution to the convection.
3. The heat transfer enhancement due to the μ-variation in the thermal developing process is pronounced.
4. The effect of k-variation on heat transfer is relatively insignificant.
5. The relative enhancement of Nusselt number, $\Delta Nu\%$, should be the function of X^+, heat flux, and the fluid property.

Acknowledgements

This investigation is currently supported by National Natural Science Foundation of China (Contract No. 90505012). The first author would like to appreciate Professor W.M. Yan for supporting his visit and research at Huafan University in Taipei.

References

[1] D.B. Tuckerman, R.F.W. Pease, High-performance heat sinking for VLSI, IEEE Electron Dev. Lett. ED-2 (5) (1981) 126–129.
[2] P. Wu, W.A. Little, Measurement of friction factors for the flow of gases in very fine channels used for microminiature Joule–Thomson refrigerators, Cryogenics 23 (5) (1983) 273–277.
[3] P. Wu, W.A. Little, Measurement of the heat transfer characteristics of gas flow in fine channel heat exchangers used for microminiature refrigerators, Cryogenics 24 (8) (1984) 415–420.
[4] J. Pfahler, J. Harley, H. Bau, J. Zemel, Liquid transport in micron and submicron channels, Sensors Actuators 22 (1–3) (1990) 431–434.
[5] M.M. Rahman, F. Gui, Experimental measurements of fluid flow and heat transfer in microchannel cooling passages in a chip substrate, in: Proceedings of the ASME International Electronics Packaging Conference, ASME, Binghamton, NY, USA, 1993, pp. 685–692.
[6] X.F. Peng, B.X. Wang, Forced convection and flow boiling heat transfer for liquid flowing through microchannels, Int. J. Heat Mass Transfer 36 (14) (1993) 3421–3427.
[7] B.X. Wang, X.F. Peng, Experimental investigation on liquid forced-convection heat transfer through microchannels, Int. J. Heat Mass Transfer 37 (suppl. 1) (1994) 73–82.
[8] X.F. Peng, G.P. Peterson, Forced convection heat transfer of single-phase binary mixtures through microchannels, Exp. Thermal Fluid Sci. 12 (1) (1996) 98–104.
[9] T.M. Harms, M. Kazmierczak, F.M. Gerner, A. Holke, H.T. Henderson, J. Pilchowski, K. Baker, Experimental investigation of heat transfer and pressure drop through deep microchannels in a (1 1 0) silicon substrate, in: Proceedings of the 1997 ASME International Mechanical Engineering Congress and Exposition, ASME, Dallas, TX, USA, 1997, pp. 347–357.
[10] T.M. Adams, S.I. Abdel-Khalik, S.M. Jeter, Z.H. Qureshi, An experimental investigation of single-phase forced convection in microchannels, Int. J. Heat Mass Transfer 41 (6–7) (1998) 851–857.
[11] C.B. Sobhan, S.V. Garimella, A comparative analysis of studies on heat transfer and fluid flow in microchannels, Microscale Thermophys. Eng. 5 (4) (2001) 293–311.
[12] B. Palm, Heat transfer in microchannels, Microscale Thermophys. Eng. 5 (3) (2001) 155–175.
[13] S.G. Kandlikar, S. Joshi, S. Tian, Effect of surface roughness on heat transfer and fluid flow characteristics at low Reynolds numbers in small diameter tubes, Heat Transfer Eng. 24 (3) (2003) 4–16.
[14] C. Yang, D. Li, J.H. Masliyah, Modeling forced liquid convection in rectangular microchannels with electrokinetic effects, Int. J. Heat Mass Transfer 41 (24) (1998) 4229–4249.
[15] E.Y.K. Ng, S.T. Tan, Computation of three-dimensional developing pressure-driven liquid flow in a microchannel with EDL effect, Numer. Heat Transfer; Part A: Applications 45 (10) (2004) 1013–1027.
[16] S.T. Tan, E.Y.K. Ng, Numerical analysis of EDL effect on heat transfer characteristic of 3-D developing flow in a microchannel, Numer. Heat Transfer; Part A: Applications 49 (10) (2006) 991–1007.
[17] A.G. Fedorov, R. Viskanta, Three-dimensional conjugate heat transfer in the microchannel heat sink for electronic packaging, Int. J. Heat Mass Transfer 43 (3) (2000) 399–415.
[18] W. Qu, I. Mudawar, Analysis of three-dimensional heat transfer in micro-channel heat sinks, Int. J Heat Mass Transfer 45 (19) (2002) 3973–3985.
[19] W. Qu, I. Mudawar, S.-Y. Lee, S.T. Wereley, Experimental and computational investigation of flow development and pressure drop in a rectangular micro-channel, J. Electron. Packaging, Trans. ASME 128 (1) (2006) 1–9.
[20] G. Gamrat, M. Favre-Marinet, D. Asendrych, Conduction and entrance effects on laminar liquid flow and heat transfer in rectangular microchannels, Int. J. Heat Mass Transfer 48 (14) (2005) 2943–2954.
[21] W. Wagner, A.K. Berlin, Properties of water and steam: the industrial standard IAPWS-IF97 for the thermodynamic properties and supplementary equations for other properties, Springer-Verlag, New York, 1998.
[22] E.N. Sieder, C.E. Tate, Heat transfer and pressure drop of liquids in tubes, Ind. Eng. Chem. 28 (1936) 1429.

[23] S.P. Mahulikar, H. Herwig, Theoretical investigation of scaling effects from macro-to-microscale convection due to variations in incompressible fluid properties, Appl. Phys. Lett. 86 (1) (2005) 014105.
[24] S.P. Mahulikar, H. Herwig, Physical effects in laminar microconvection due to variations in incompressible fluid properties, Phys. Fluids 18 (7) (2006) 073601.
[25] F.S. Sherman, Viscous Flow, McGraw-Hill, New York, 1990.
[26] R.B. Bird, W.E. Stewart, E.N. Lightfoot, Transport Phenomena, second ed., John Wiley & Sons, New York, 2002.
[27] V.S. Arpaci, P.S. Larsen, Convection Heat Transfer, Prentice-Hall, London, 1984.
[28] R.K. Shah, A.L. London, Laminar Flow Forced Convection in Ducts: A Source Book for Compact Heat Exchanger Analytical Data, Academic Press, New York, 1978.